Highly Negative Electric Probes in a Flowing Continuum Plasma

P.C.T. deBoer* and T.S. David†
Cornell University, Ithaca, N.Y.

The general problem of an electric probe in a flowing continuum plasma is solved using perturbation theory, together with the method of matched asymptotic expansions. The small parameter used is the inverse of the dimensionless probe potential. The lowest order results yield a quasineutral region in which the ion concentration is constant, and an ion sheath region in which the electron density is zero. The electric potential and the electric field are zero at the edge of the sheath region. The remaining problem consists of solving the sheath equations. A solution is found for spherical and cylindrical probes in the case that the sheath is thin compared with the radius of the probe, but thick compared with the viscous boundary layer. For sheaths that are not thin compared with the probe radius, an iterative method of solution is proposed. The results are presented as a one-parameter family of curves. It is shown that there exists a limiting current, which obtains when the ion density around the probe remains essentially equal to the freestream value. The theoretical results obtained are in fair agreement with available experimental data. Attention is given to other theoretical results, as well as to various improvements needed for further progress.

Nomenclature

D = diffusion coefficient
e = electronic charge
h_i = $(\epsilon_n kT_i/N_{i\infty}e^2)^{1/2}$ = ion Debye length
I = physical current to probe
j_j = nondimensionalized ion current density
J_j = $eN_\infty U_\infty j_j$ = physical current density
$\mathcal{J}$ = nondimensionalized current to probe, defined by Eqs. (32) or (47)
k = Boltzmann's constant
ℓ_p = length of cylindrical probe
M = Mach number
n = N/N_∞ = nondimensionalized number density
N = number density
p_j = coordinates perpendicular to and along transition surface
qn = quasineutral region
r = radial distance coordinate
$ReSc_i$ = $2U_\infty r_p/D_i$ = product of Reynolds number based on probe diameter and ion Schmidt number
R_i = $\frac{1}{2}ReSc_i h_i/r_p = U_\infty h_i/D_i$ = ion Reynolds number based on ion Debye length
s = sheath region
T = temperature
U_j = flow velocity of neutral component
v_j = U_j/U_∞ = nondimensionalized flow velocity
V = electric potential
x_j = distance coordinate
α = $180° - \theta$; $\alpha = r_s/r_0$ in Sec. V
β = $D_i/(\tau D_e)$
δ = $\rho_s - \rho_p$ = sheath thickness
ϵ_n = dielectric constant of neutral component
ϕ = V/V_p = nondimensionalized electric potential
$\tilde{\psi}$ = $\tau^{-1}\ell_n\tilde{n}_0 + \tilde{\phi}_2$, defined following Eq. (18)
μ = $R_i(\tilde{n}_0/\omega)^{1/2}\nu$
ν = stretched coordinate perpendicular to transition surface, defined following Eq. (14)
ω = $-eV_p/kT_i$ = nondimensionalized probe potential
Ω = $\omega h_i^2/r_p^2 = \omega R_i^{-2}\rho_p^{-2}$ = sheath thickness parameter, see Eqs. (34) and (49)
ρ = $r/(h_i R_i)$ = nondimensionalized radial coordinate
$1/\rho_p$ = $\frac{1}{2}ReSc_i h_i^2/r_p^2$
τ = T_i/T_e
θ = angular coordinate (see Fig. 1)
ξ_j = $x_j/(h_i R_i)$, nondimensionalized coordinate

Subscripts

e = electrons
i = ions
j = 1,2,3, denoting x, y, or z coordinates, respectively; summation convention applies to j
k = 1,2,3, as j
L denotes limiting value
ℓ_n denotes logarithmic term in expansion
n = neutral species
p = probe
t = transition surface
ν = component in direction of ν
∞ = undisturbed region far from probe
$0,1,2\ldots$ = order of expansion quantity
1,2, or *3* denote coordinates when following ξ or p

Superscripts

$\tilde{}$ = transition region
$\hat{}$ = ion diffusion layer near probe

Received July 21, 1976; revision received Feb. 15, 1977.
Index categories: Plasma Dynamics and MHD; Atomic, Molecular, and Plasma Properties.

*Professor, Sibley School of Mechanical and Aerospace Engineering. Associate Fellow AIAA.
†Teaching Assistant.

I. Introduction

THE theory of electric probes in flowing continuum plasmas is needed for the interpretation of experimental data. Much work has been done on the subject, especially for the case of plane probes that are flush with the wall. A review of this work has recently been given by Chung, Talbot, and Touryan,[1] who included an extensive list of references.

The present paper is concerned primarily with spherical probes and with cylindrical probes perpendicular to the flow, for the case that the ion sheath thickness is large compared with the viscous boundary layer. The sheath thickness may be either small or not small compared with the probe diameter. First, the problem of an electric probe in a flowing continuum plasma is taken up in general. This problem has previously been considered by Lam.[2] We simplify the basic equations by using perturbation theory, together with the method of

matched asymptotic expansions.[3-5] This approach is analogous to that followed in Ref. 6 for a flat plate probe in a flowing plasma, and in Ref. 7 for a spherical probe in a quiescent plasma. The small parameter used is the inverse of the dimensionless probe potential. Another possible choice, not worked out in detail here, would be the ratio of ion to electron diffusion coefficient.[6] The equations are nondimensionalized using the ion Debye length. It is found that the lowest order equations yield two distinct regions. In one of these (the quasineutral region), the electric potential is zero, while the electron density equals the ion density. In the other region (the ion sheath region), the electron density equals zero, while the electric potential is nonzero (all of these results apply to lowest order quantities). An explicit solution is found for the transition region separating the two main regions. This solution provides the boundary conditions under which the equation for the ion sheath region must be solved. The boundary condition along the wall follows from considering the "ion diffusion layer" near the wall, first described by Su and Lam.[8]

The general problem of finding the solution for the ion sheath is discussed. Detailed solutions are presented for spherical and cylindrical probes, for the case that the plasma flow about these probes may be described by the potential flow equations.

II. General Theory

We consider the steady flow of a slightly ionized continuum gas, with all ions singly charged and of the same species. The rates of production and recombination of ions and electrons are assumed to be negligibly small. The electron temperature T_e and the ion temperature T_i are assumed to be constant throughout the flowfield, as are the diffusion coefficients D_e and D_i. Following Refs. 2 and 6, we then have

$$\frac{\partial j_j}{\partial \xi_j} \equiv \frac{\partial}{\partial \xi_j}(n_i v_j) - \frac{\omega}{R_i^2}\frac{\partial}{\partial \xi_j}\left(\frac{1}{\omega}\frac{\partial n_i}{\partial \xi_j} - n_i\frac{\partial \varphi}{\partial \xi_j}\right) = 0 \quad (1)$$

$$\beta\tau\frac{\partial}{\partial \xi_j}(n_e v_j) - \frac{\omega}{R_i^2}\frac{\partial}{\partial \xi_j}\left(\frac{1}{\omega}\frac{\partial n_e}{\partial \xi_j} + n_e\tau\frac{\partial \varphi}{\partial \xi_j}\right) = 0 \quad (2)$$

$$\frac{\omega}{R_i^2}\frac{\partial^2 \varphi}{\partial \xi_j^2} = n_i - n_e \quad (3)$$

The neutral flow velocity v_j is considered to be given. The boundary conditions under which we want to solve these equations are:

far from probe: $n_i = n_e = 1 \varphi = 0$ (4a)

at probe: $n_i = n_e = 0, \quad \varphi = 1$ (4b)

We are interested in the case of a highly negative probe, i.e. in the limit $\omega \to \infty$. Because we want to retain the influence of flow effects, we further require that $\omega/R_i^2 = 0(1)$. It follows that $R_i \to \infty$. Furthermore, we note that the ion diffusion coefficient D_i is much smaller than the electron diffusion coefficient D_e, so that β is very small. For the limiting case $\beta = 0$, Eq. (2) has the solution

$$n_e = \exp(-\omega\tau\varphi) \quad (5)$$

where the multiplicative constant was set equal to 1 in view of conditions (4a). In the case of flow over a flat plate[6] and of a spherical probe without flow,[7] it was shown that Eq. (5) is the unique solution of Eq. (2). In the present, more general case, no proof of uniqueness is available. However, it is plausible that Eq. (5) is the appropriate solution of Eq. (2) in the limit $\beta = 0$.

We expand as follows

$$\varphi = \varphi_0 + \omega^{-1/2}\varphi_1 + \omega^{-1}\varphi_2 + \ldots \quad n_i = n_0 + \omega^{-1/2} n_1 + \ldots$$

$$n_e = n_{e0} + \omega^{-1/2} n_{e1} + \ldots \quad j_j = j_{0j} + \omega^{-1/2} j_{1j} + \ldots \quad (6)$$

and equate terms of the same order in ω in Eqs. (1,3, and 5). For $\phi_0 = 0$, the lowest order results are

$$(\partial/\partial \xi_j)(n_0 v_j) = 0 \quad (qn) \quad (7)$$

$$n_0 = n_{e0} = \exp(-\tau\varphi_2) \quad (qn) \quad (8)$$

The region where these results apply is called the quasineutral (qn) region, in view of the condition $\phi_0 = 0$. In fact, we also have $\phi_1 = 0$ in this region, because otherwise n_0 would be identically zero. Since the neutral component satisfies the equation $(\partial/\partial \xi_j)(n_n v_j) = 0$, the solution of Eq. (7) may be given in terms of the ion concentration n_0/n_n:

$$n_0/n_n = \text{constant} \quad (qn) \quad (9)$$

For given n_n, Eq. (9) provides n_0, while Eq. (8) yields ϕ_2.

For $\phi_0 \neq 0$, the lowest order results are

$$\frac{\partial}{\partial \xi_j} j_{0j} = \frac{\partial}{\partial \xi_j}\left(v_j \frac{\partial^2 \varphi_0}{\partial \xi_k^2}\right) + \frac{\omega}{R_i^2}\frac{\partial}{\partial \xi_j}\left(\frac{\partial \varphi_0}{\partial \xi_j}\frac{\partial^2 \varphi_0}{\partial \xi_k^2}\right) = 0 \text{ (s)} \quad (10)$$

$$n_0 = \frac{\omega}{R_i^2}\frac{\partial^2 \varphi_0}{\partial \xi_j^2} \quad \text{(s)} \quad (11)$$

$$n_{e0} = 0 (= n_{e1} = n_{e2} = \ldots) \quad \text{(s)} \quad (12)$$

These results apply to the ion sheath region near the probe. Between the ion sheath and the quasineutral region there is a transition surface. In order to find the boundary conditions under which Eq. (10) must be solved, it is necessary to consider this transition surface in more detail. The following treatment is a generalization of that presented in Ref. 6.

We introduce the orthogonal coordinate system (p_1, p_2, p_3), where p_1 denotes distance perpendicular to the transition surface, counted positive in the direction from the sheath to the quasineutral region, while p_2 and p_3 are distance coordinates along the surface. Equations (1) and (3) then become

$$\frac{\partial}{\partial p_j}(\tilde{n}_i v_{pj}) - \frac{\omega}{R_i^2}\frac{\partial}{\partial p_j}\left(\frac{1}{\omega}\frac{\partial \tilde{n}_i}{\partial p_j} - \tilde{n}_i\frac{\partial \tilde{\varphi}}{\partial p_j}\right) = 0 \quad (13)$$

$$\frac{\omega}{R_i^2}\frac{\partial^2 \tilde{\varphi}}{\partial p_j^2} = \tilde{n}_i - \tilde{n}_e, \quad (14)$$

with v_{pj} denoting the component of the vector $\bar{v}$ in the direction of p_j. We now set $p_i = \nu/\omega^{1/2}$, and use the expansions (6) together with $v_{pj} = \tilde{v}_0 + \omega^{-1/2}\tilde{v}_1 + \ldots$, where $\tilde{v}_0 = v_{pl}(0, p_2, p_3)$, $\tilde{v}_1 = \nu(\partial v/\partial p_1)(0, p_2, p_3)$, etc.

To orders ω and $\omega^{1/2}$, Eq. (14) yields $\partial^2 \phi_0/\partial \nu^2 = 0$ and $\partial^2 \tilde{\phi}_1/\partial \nu^2 = 0$, respectively. Matching with the outer region requires

$$\tilde{\varphi}_0 = 0, \qquad \tilde{\varphi}_1 = 0 \quad (15)$$

Similarly, Eq. (13) yields to order $\omega^{1/2}$: $(\partial/\partial \nu)(\tilde{j_{0\nu}}) = 0$, where $j_{0\nu} = \tilde{n}_j \tilde{v}_0$ is the component of j_0 in the direction of ν. With both $\tilde{n}_0 \tilde{v}_0$ and $\tilde{v}_0$ independent of ν, it follows that $\tilde{n}_0$ must be independent of ν:

$$\tilde{n}_0 = \tilde{n}_0(p_2, p_3) \quad (16)$$

Next, we consider Eq. (13) to order ω^0

$$\tilde{v}_0\frac{\partial\tilde{n}_1}{\partial\varphi}+\frac{\partial}{\partial p_2}(\tilde{n}_0 v_{p2})+\frac{\partial}{\partial p_3}(\tilde{n}_0\tilde{v}_{p3})+\tilde{n}_0\frac{\partial\tilde{v}_1}{\partial\nu}$$

$$+\frac{\omega}{R_i^2}\tilde{n}_0\frac{\partial^2\tilde{\varphi}_2}{\partial\nu^2}=0 \tag{17}$$

which must be solved for $\tilde{n}_1$ after $\tilde{\phi}_2$ is known. The latter quantity follows from Eq. (14) to order ω^0:

$$-\frac{\omega}{R_i^2}\frac{\partial^2\tilde{\varphi}_2}{\partial\nu^2}=\tilde{n}_0-\tilde{n}_{e0} \tag{18}$$

Defining $\tilde{\psi}\equiv\tau^{-1}\ell_n\,\tilde{n}_0+\tilde{\phi}_2$, this may be written

$$\partial^2\tilde{\psi}/\partial\mu^2=1-\exp(-\tau\tilde{\psi}), \tag{19}$$

where $\mu=R_i(\tilde{n}_0/\omega)^{1/2}\nu$, and where use was made of Eq. (5). The solution of Eq. (19) is

$$2^{-1/2}\int_0^{\tilde{\psi}}d\psi[\psi+\tau^{-1}\exp(-\tau\psi)+C_1]^{-1/2}=\pm\mu+C_2, \tag{20}$$

where C_1 and C_2 may depend on p_2 and p_3, but not on μ. Matching with the quasineutral region requires that $\tilde{\psi}\to 0$ as $\mu\to\infty$, so that the negative sign must be taken, while $C_1=-\tau^{-1}$. This yields

$$\tilde{\psi}\sim\exp(-\tau^{1/2}\mu+C_2)\ \text{ as }\ \mu\to\infty \tag{21}$$

Furthermore,

$$\tilde{\psi}\sim\tfrac{1}{2}\mu^2+A\mu+b\quad\text{as}\quad\mu\to-\infty, \tag{22}$$

where A and B depend on C_2 and τ; in principle, they can be determined by numerical integration of Eq. (20). For present purposes we need the first term of Eq. (22), only, which yields for the 1- term expansion in sheath variables of the 3-term transition tesult

$$\tilde{\varphi}=\tilde{\varphi}_0+\omega^{-1/2}\tilde{\varphi}_1+\omega^{-1}\varphi_2+\ldots\sim\tfrac{1}{2}(R_i^2/\omega)\tilde{n}_0 p_1^2$$

Matching this with the 3-term transition expansion of the 1-term sheath result yields

$$\varphi_0(0,p_2,p_3)=0\quad(\partial\varphi_0/\partial p_1)(0,p_2,p_3)=0 \tag{23}$$

$$\frac{\omega}{R_i^2}\frac{\partial^2\varphi_0}{\partial p_1^2}(0,p_2,p_3)\equiv n_0(0,p_2,p_3)\,|_s$$

$$=\tilde{n}_0(p_2,p_3)=n_0(0,p_2,p_3)\,|_{qn} \tag{24}$$

The last equality of Eq. (24) is based on Eq. (16), which also provides an alternative way to derive the next to last equality of Eq. (24). Equations (23) and (24) provide the boundary conditions along the transition surface under which Eq. (10) must be solved: both the electrical potential ϕ_0 and electric field $\partial\phi_0/\partial p_1$ are zero, while the Laplacian $\partial^2\phi_0/\partial\xi_j^2$ is prescribed by the quasineutral solution.

As first pointed out by Su and Lam,[8] there also is a transition layer near the probe surface. This layer is an "ion diffusion layer." Its solution can be found by introducing a scaled coordinate $\hat{x}=\omega(\xi_1-\xi_{1p})$ perpendicular to the probe, with $\hat{x}=0$ at the probe.[6] Using the expansions

$$\hat{\varphi}=\hat{\varphi}_0+\omega^{-1}\hat{\varphi}_1+\ldots,\ \hat{n}_i=\hat{n}_0+\omega^{-1}\hat{n}_1+\ldots \tag{25}$$

it is found that

$$\hat{\varphi}_0=1,\quad d\hat{\varphi}_1/d\hat{x}=C_1, \tag{26}$$

where C_1 is a negative constant to be determined from matching with the ion sheath region. Furthermore

$$\hat{n}_0=\hat{n}_0(\hat{x}=\infty)+[\hat{n}_0(\hat{x}=0)-\hat{n}_0(x=\infty)]\exp(\hat{x}\,d\hat{\varphi}_1/d\hat{x}) \tag{27}$$

The ion diffusion layer has a thickness of order ω^{-1}, and can satisfy a "slip condition" on n_0 at the probe, besides the present condition $n_0=0$. It also can satisfy any condition on $\hat{n}_0$ at $\hat{x}=\infty$. As a result, the boundary condition at the probe under which Eq. (10) must be solved simply becomes $\phi_0=1$.

The problem now has been reduced to find the solution of Eq. (10) under the boundary condition $\phi_0=1$ along the probe surface, together with boundary conditions (23) and (24), where n_0 $(0, p_2, p_3)$ is given by Eq. (9). The coordinates of the transition surface are not known a priori, and their determination is an important part of the problem. A solution procedure for spherical and cylindrical probes is described in the following sections.

Besides the expansion in powers of $\omega^{1/2}$ considered, it is possible to expand in powers of β, taking the limit $\omega\to\infty$, $R_i\to\infty$, $\omega^{1/2}/R_i=0(1)$. To lowest order the equations and boundary conditions for the ion sheath are the same as obtained above. The results suggest that the electron density in the ion sheath is of order β, rather than exponentially small in ω, as indicated by Eq. (5) (see also Ref. 6.).

Still another limit that can be considered is $\beta\to 0$, $\omega\to\infty$, $R_i=0(1)$. Introducing the new spatial coordinate $\eta_j=\bar{x}_j/(h_i\omega^{1/2})$, setting $\beta=0$ and expanding in powers of $\omega^{-1/2}$ then reproduces Eqs. (7, 10, and 11), except that ξ is replaced by η and ω/R_i^2 by 1, while the convection term (i.e. the term with v_j) in Eq. (10) has disappeared. Further analysis shows that when applied to practical problems with given values of ω and R_i, the results obtained this way are a special case of the previous results. This special case is obtained by allowing the numerical value of R_i to be of order 1. The convection term in Eq. (10) then becomes very small numerically compared with the electric mobility term, while the remaining equations are unchanged. It may be concluded that the previous results can be applied to practical problems even when R_i is of order 1.

III. Application to Spherical Probes

We represent v_j by the inviscid, incompressible potential flow around a sphere (see e.g. Ref. 9, p. 123):

$$v=(1-\rho_p^3/\rho^3)\cos\theta\boldsymbol{e}_k-(1+\tfrac{1}{2}\rho_p^3/\rho^3)\sin\theta\boldsymbol{e}_\theta \tag{27}$$

where $\boldsymbol{e}_\rho$ and $\boldsymbol{e}_\theta$ are unit vectors in the directions determined by $\theta=$constant and $\rho=$constant, respectively (Fig. 1). Of course, the actual flow around a sphere is quite different from the potential flow assumed, especially near the rearward part of the sphere. However, most of the ions are collected on the forward part, and Eq. (27) probably is sufficiently accurate for most practical purposes provided the viscous boundary layer is thin compared with the sheath. The latter condition must be checked before the results can be applied to any particular case. Substituting Eq. (27) into Eq. (10) and using Eq. (11) as well as the relation $\partial v_j/\partial\xi_j=0$, we obtain

$$\left[\left(1-\frac{\rho_p^3}{\rho^3}\right)\cos\theta+\frac{\omega}{R_i^2}\frac{\partial\varphi_0}{\partial\rho}\right]\frac{\partial n_0}{\partial\rho}+\frac{1}{\rho}\left[-\left(1+\frac{\rho_p^3}{2\rho^3}\right)\sin\theta\right.$$

$$\left.+\frac{\omega}{R_i^2\rho}\frac{\partial\varphi_0}{\partial\theta}\right]\frac{\partial n_0}{\partial\theta}=-n_0^2 \tag{28}$$

The solution of Eq. (28) for n_0 in terms of derivatives of ϕ_0 is given by the method of characteristics (see e.g. Ref. 10, pp. 302-310) as[11]

$$n_0=(1+t)^{-1} \tag{29}$$

where use was made of Eq. (24) with $n_0(0, p_2, p_3)=1$, and where t is a parameter along the characteristic lines, with $t=0$ at the sheath edge. The characteristic lines are given by

$$d\rho/dt=(1-\rho_p^3/\rho^3)\cos\theta+\omega R_i^{-2}\partial\varphi_0/\partial\rho$$

$$d\theta/dt=-\rho^{-1}(1+\tfrac{1}{2}\rho_p^3/\rho^3)\sin\theta+\omega R_i^{-2}\rho^{-2}\partial\varphi_0/\partial\theta \quad (30)$$

It can easily be verified that these lines are the ion streamlines. The lowest order current density at the probe is given by

$$j_p=-\omega R_i^{-2}(n_0\partial\varphi_0/\partial\rho)_p \quad (>0) \quad (31)$$

while the lowest order current collected by the probe is

$$\mathcal{J}=2\pi\rho_p^2\int_0^\pi j_p(\theta)\sin\theta d\theta \quad (32)$$

where the subscript zero has been dropped from j and $\mathcal{J}$.

In order to solve Eqs. (29, 30, and 11), we use the following iterative scheme. First, we take $n_0=1$ and solve Eq. (11) for $\partial\phi_0/\partial\rho$. This provides a limiting value $\mathcal{J}_L\equiv 4\pi\rho_0^2 j_{pL}$ for the total dimensionless current collected by the probe. Using the result obtained for $\partial\phi_0/\partial\rho$, Eqs. (30) can be solved for $d\rho/dt$ and $d\theta/dt$. This provides the ion streamlines. By tracing the ion streamline leading to the ion stagnation point back to the sheath edge (see Fig. 2), an improved value can be obtained for the total current $\mathcal{J}$ collected by the probe. In principle, the results can also be used to find a new function $n_0(\rho,\theta)$, so that the process can be repeated. However, we have not carried out any further iterations.

The limiting result $\mathcal{J}_L$ is given by

$$\mathcal{J}_L=(4\pi/3)\rho_p^3(-1+\rho_s^3/\rho_p^3) \quad (33)$$

where the radius ρ_s of the sheath follows from

$$\Omega\equiv\omega R_i^{-2}\rho_p^{-2}=(1/6)(-1+\rho_s/\rho_p)^2(1+2\rho_s/\rho_p) \quad (34)$$

A plot of $-1+\rho_s/\rho_p$ as function of Ω is shown in Fig. 3. The total current $\mathcal{J}$ after the first iteration is givey by $\mathcal{J}=\int_S v_j dS_j$, where S is the area of the transition surface enclosed by the streamlines leading to the ion stagnation point (see Fig. 2). These streamlines were determined by numerical computation. The results consist of a one-parameter family of curves, which can be plotted in various ways. One possibility is shown in Fig. 4, where $\mathcal{J}/\mathcal{J}_L$ is plotted as function of $1/\rho_p(\equiv\tfrac{1}{2}Reh_i^2/r_p^2)$ for various values of the parameter Ω (0.01, 0.1, 1, 10, 100). It can be seen that $\mathcal{J}/\mathcal{J}_L<1$ under all conditions, with $\mathcal{J}/\mathcal{J}_L\to 1$ as $1/\rho_p\to\infty$ for all Ω. This behavior can be understood by noting that both the ion density n_{op} and the electric field $(\partial\phi_0/\partial\rho)_p$ at the probe are maximum for $n_0=1$ throughout the sheath, which is just the limit considered in calculating $\mathcal{J}_L$. This limit obtains when convective effects dominate over electric effects, i.e., when $\omega R_i^{-2}\rho_p^{-1}<<1$ [cf. Eqs. (28) and (30)], or when $1/\rho_p>>\Omega$. For small values of $1/\rho_p$, $\mathcal{J}/\mathcal{J}_L$ is much smaller than unity. The current collected in this limit simply is the current entering the sheath, and is given by $\mathcal{J}\mid\mathcal{J}_L=3/(4\rho_s)$, with ρ_s following from Eq. (34). With electric effects dominating over convective effects, the ion density in the rearward portion of the sheath is zero after this iteration. This indicates that the result obtained is a lower bound to the actual result.

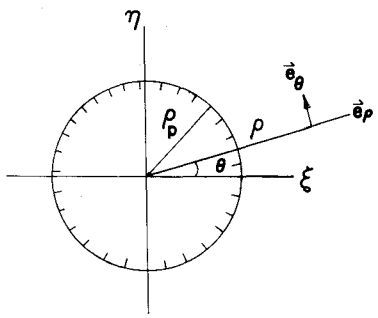

Fig. 1 Coordinate system for spherical and cylindrical probes.

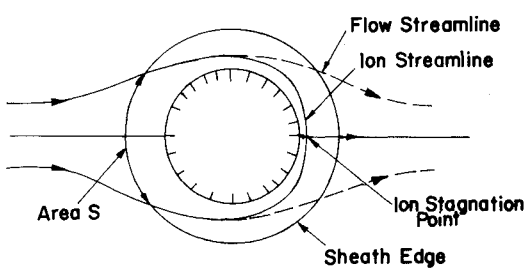

Fig. 2 Flow pattern around probe in first iteration.

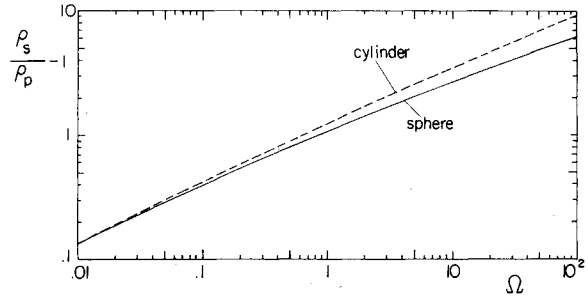

Fig. 3 Ratio of sheath radius ρ_s to probe radius ρ_p as function of the parameter Ω, for spherical and cylindrical probes with $n_0=1$ in the sheath.

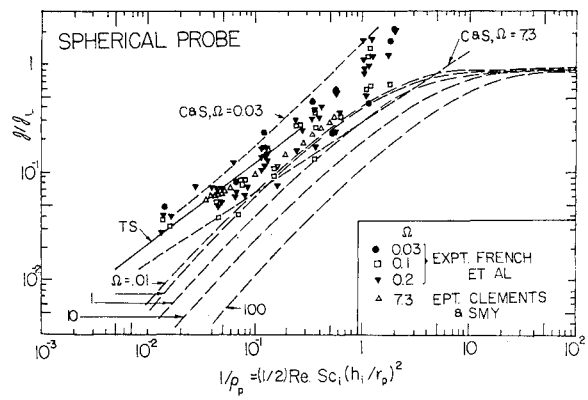

Fig. 4 $\mathcal{J}/\mathcal{J}_L$ as function of $1/\rho_p$ for spherical probe, at various values of the parameter Ω. TS (thin sheath) results based on Eq. (41), C&S results on Ref. 15, expt. French et al. on Ref. 13, expt. Clements and Smy on Ref. 15.

Special Case: Thin Sheath

It is possible to solve Eqs. (29, 30, and 11) along the streamline $\theta=\pi$ for the special case that the sheath is thin compared with the probe radius ($\rho_s-\rho_p<<\rho_p$). For this case, Eqs. (11) and (29) yield $(1+t)^{-1}=\omega R_0^{-2}d^2\phi_0/d\rho^2$, while the first of Eqs. (30) becomes

$$d\rho/dt=-3(\rho-\rho_p)/\rho_p+\omega R_i^{-2}d\varphi_0/d\rho \quad (<0)$$

Differentiating the latter relation with respect to ρ_1 and noting that $t=t(\rho)$, we find after some algebra

$$(\rho-\rho_p)/(\rho_s-\rho_p)=(1+t+\rho_p/3)\exp(-3t/\rho_p)-\rho_p/3 \quad (35)$$

For $\rho_p >> 1$, this equation yields $t_p \approx (2\rho_p/3)^{1/2}$. Since $0 \leq t \leq t_p$, the right hand side of Eq. (35) in this case may be written as $1 - 3t^2/(2\rho_p)$. Solving for t, substituting the result in the equation for $\omega R_i^{-2}\, \mathrm{d}^2\, \phi_0/\mathrm{d}\rho^2$, and integrating twice leads to the results

$$\delta(\theta-\pi) \equiv \rho_s(\theta=\pi) - \rho_p \approx (3/8)^{1/4} \rho_p^{5/4} \Omega^{1/2} \tag{36}$$

$$j(\theta=\pi) \leq 3^{5/4} 2^{-3/4} \rho_p^{1/4} \Omega^{1/2} \approx (9/8)\, \rho_p^4 \Omega^2 [\delta(\theta=\pi)]^{-3}, \tag{37}$$

where the subscripts 0 and p were dropped from j. These relations are identical to those obtained for a one-dimensional, space-charge limited sheath.[12] This is understandable because in the limit considered ($\rho_p >> 1$), electric effects dominate over convective effects in most of the sheath.

The dominance of electric effects over convective effects for $\rho_p >> 1$ can be used to find an approximate solution for all θ. To this purpose, we resort to the quasi-one-dimensional method of Ref. 12. The basic idea is to take Eq. (37) as a general relation between $j(\theta)$ and $\delta(\theta) \equiv \rho_s(\theta) - \rho_p$, and to use as a second equation the continuity of j at the edge of the sheath. The applicability of this method to spherical and cylindrical probes was previously noted by French et al,[13] who used additional approximations to arrive at a result for the cylindrical case. For the spherical case, the continuity equation for j at the edge of the sheath is

$$j(\alpha) = (3\delta_s/\rho_p)\cos\alpha + (3/2\rho_p)\sin\alpha\, \mathrm{d}\delta_s/\mathrm{d}\alpha, \tag{38}$$

where $\alpha \equiv \pi - \theta$. Combining this with the relation $j(\alpha) = (9/8)\rho_p^4 \Omega^2 \delta^{-3}$, and using Eq. (37) leads to

$$\mathrm{d}\gamma/\mathrm{d}\alpha = -8\gamma(\gamma - \cos\alpha)/\sin\alpha \tag{39}$$

where $\gamma \equiv [j/\alpha)/j(0))]^{4/3} = [\delta(0)/\delta(\alpha)]^4$. We have solved Eq. (39) by numerical integration, starting at $\alpha = 0$. The first step was found from the expression $\gamma = 1 - 2\alpha^2/5\ldots$, valid for small α. The result obtained is plotted in Fig. 5. It is clear that most of the ion current is collected on the forward part of the probe. Near $\alpha = \pi$ ($\theta = 0$), the thin sheath assumption breaks down, but the resulting error in the total current collected is of little consequence. The total current is given by $\mathcal{J} = j(0)\, 2\pi\rho_p^2 \int_0^\pi [j(\alpha)/j(0)] \sin\alpha \mathrm{d}\alpha$. Numeical integration of the result shown in Fig. 5 yielded

$$\mathcal{J} = 12.0 \rho_p^{9/4} \Omega^{1/2} \quad \text{(thin sheath)} \tag{40}$$

For the thin sheath case under consideration, (33) becomes $\mathcal{J}_L = 4\pi\rho_p^3(2\Omega)$, so that

$$\mathcal{J}/\mathcal{J}_L = 0.676 \rho_p^{-3/4} \quad \text{(thin sheath)} \tag{41}$$

This result is represented on Fig. 4 by the line marked "TS". It may be regarded as the definitive result for the case $\Omega << 1$, $1/\rho_p << 1$. As was to be expected, it lies above the results of the first iteration shown by the solid lines, which provide a lower bound to the actual result.

For $\rho_p << 1$, Eq. (35) yields $t_p \approx (\rho_p/3)\ell n(3/\rho_p)$, which is much smaller than unity. It follows that $n_{op} \approx 1$, so that $n_0 \approx 1$ throughout the sheath. As a consequence, the thin sheath limit in this case is identical to the limiting case considered previously, for which $\mathcal{J} = \mathcal{J}_L$.

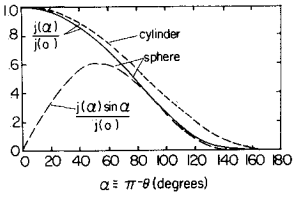

Fig. 5 Current density $j(\alpha)/j(0)$ for sphere and cylinder, and weighted current density $j(\alpha)\sin\alpha/j(0)$ for sphere, as function of α (thin sheath).

Application of Results

The present theory can be used to evaluate ion density from experimental data, provided the free stream velocity U, the temperature T_i, the ion diffusion coefficient D_i and the probe potential V_p all are known. To this purpose, it is convenient to use a plot in which the vertical and horizontal coordinates are

$$\mathcal{J}\Omega^{-2}\rho_p^{-3} Ier_p/(\epsilon_0 k T_i \omega^2) \tag{42}$$

$$(\Omega\rho_p)^{-1} = \tfrac{1}{2} ReSc_i \omega^{-1}, \tag{43}$$

respectively, while curves are plotted for constant

$$\Omega \equiv \omega h_i^2/r_p^2 = \omega\epsilon_0 k T_i/(N_0 e^2 r_p^2) \tag{44}$$

With the right hand sides of Eqs. (42) and (43) both known, such a plot can be used to determine Ω, and hence N_0. Alternatively, use can be made of the analytical thin sheath result based on Eq. (40)

$$\Omega = 2.75(\Omega\rho_p)^{-1}(\mathcal{J}\Omega^{04}\rho_p^{-3})^{-4/3} \tag{45}$$

in combination with Eqs. (42) and (43).

One of the conditions which must be verified before applying the present theory is that the viscous boundary layer must be thin compared with the thickness of the sheath. It can be shown that this condition is satisfied at the stagnation point provided $\rho_p^{-1} >> 22\omega^{-2}$ in the case of a spherical probe, or $\rho_p^{-1} >> 15\omega^{-2}$ in the case of a cylindrical probe.

Influence of Compressibility and Ion Production

The preceding results have been derived under the restrictive assumption of incompressible flow. In many cases of practical interest, it is desired to measure ion density in flows that are compressible. The present theory cannot easily be extended to such flows. However, it is possible to investigate the effects of compressibility in a qualitative way. For example, consider the case of supersonic flow. The plasma in the vicinity of the probe then has passed through a bow shock. A simple method for estimating the influence of compressibility effects consists of taking conditions behind the bow shock as the appropriate undisturbed flow conditions. Given the measured current I, it can easily be shown that the inferred quantity $\mathcal{J}/\mathcal{J}_L$ is proportional to $U_\infty^2 T_\infty D_\infty^{-1} (-1 + \rho_s^3/\rho_{p2}^3)$. Here, ρ_s/ρ_p follows from Eq. (34), and depends on the value of Ω. The latter quantity is proportional to U_∞, while $1/\rho_p$ is proportional to $U_\infty T_\infty/D_\infty$. Application to shock tube flows, in which the free stream is only slightly supersonic ($M < 1.5$, say), shows that $\mathcal{J}/\mathcal{J}_L$ is practically constant across the bow shock, while $1/\rho_p$ decreases by only a small amount. We take this to indicate that the evaluation of experimental data taken in such flows is not much affected by compressibility. For large freestream Mach numbers the changes in $1/\rho_p$ and $\mathcal{J}/\mathcal{J}_L$ become more severe, and the resulting error in the inferred ion density may no longer be inconsequential.

Another effect left out of account so far is that of ion production in the vicinity of the probe. Such production can arise because of the absence of electrons in the ion sheath ("chemical ionization"), and also because of the higher temperatures caused by compressibility effects ("thermal ionization"). The absence of electrons means that ion-electron recombination reactions do not occur. The rate of ion production may be characterized by the production parameter

$$P \equiv a h_i^2/(N_\infty D_\infty) = (a r_p/N_\infty U_\infty)(1/\rho_p),$$

where a is the rate of ion production per unit volume.[14,11] The quantity N_∞/a is a characteristic relaxation time for ionizaton. In the limiting case $1/\rho_p << \Omega$ (electric effects in the sheath dominant over convective effects), it can be shown that for N_∞/a constant and sufficiently small

$$\mathcal{J}/\mathcal{J}_L = P(-1+r_s^3/r_p^3)/(-1+\rho_s^3/\rho_p^3)_L,$$

where r_s/r_p follows from

$$\Omega = (1/6)P^{1/2}(-1+r_s/r_p)^2(-1+2r_s/r_p),$$

while $(-1+\rho_s^3/\rho_p^3)_L$ follows from Eq. (34). In this limiting case the ion density in the sheath is constant, and equals $N_\infty P^{1/2}$.

Qualitative estimates indicate that for $1/\rho_p$ and Ω both of order 1, the increase of $\mathcal{J}/\mathcal{J}_L$ caused by production is of the order of P. Thus, the influence of chemical ionization becomes quite pronounced when P is of order 1 or larger. It seems plausible that the influence of thermal ionization in the quasineutral region generally is of the same order as that of chemical ionization. However, further investigation of these effects is considered outside the scope of this paper.

Comparison with Experimental Data

Experimental data taken under conditions where the present theory should be applicable were reported by Clements and Smy.[15] These data were obtained by moving a spherical electric probe at known velocity through a flame. The electron density was measured using microwave techniques. The value of ω was about 710, while $h_i/r_p \approx 0.1$, $\Omega \approx 7.3$, $\rho_s/\rho_p \approx 3.4$, $ReSc_i \approx 7 \rightarrow 110$, $R_i \approx 0.36 \rightarrow 5.6$. The maximum value of the Mach number was about 0.1. The data plotted in Fig. 3 of Ref. 15 are included in the present Fig. 4. They are seen to fall between the result of the first iteration and the thin sheath result. In this sense, the agreement is as good as could be expected. The theoretical results marked "C&S" are discussed in Sec. V.

Experiments with spherical probes in a continuum flow under conditions where the sheath is thick compared with the viscous boundary layer were also reported by French et al.[13] The electron density was measured with microwave instrumentation. The data were obtained using a shock tube, with flow Mach numbers ranging from 1.1 to 1.4. Consequently, the flow around the probe was compressible. As indicated in preceding subsection, the effects of compressibility on the values derived for $\mathcal{J}/\mathcal{J}_L$ and $1/\rho_L$ are expected to be small. We have found it interesting, therefore, to compare the present theory also with the experimental results of Ref. 13. To this purpose, the data plotted in Fig. 4 of Ref. 13 were included in the present Fig. 4. The experimental values of ω ranged from 7 to 70, of Re from 8 to 10^3, and of h_i/r_p from 0.04 to 0.09. For the conversion to present variables, the value of h_i/r_p was needed for each datum point; this value was approximated as 0.06. The resulting range of R_i was from 0.24 to 30. Similarly, from the groups of data with $7 < \omega < 13$, $21 < \omega < 38$ $38 < \omega < 70$, the ω values were approximated as 9.5, 28 and 52, respectively. It can be seen from Fig. 4 that the resulting groups with average Ω values of 0.03, 0.1 and 0.2 are correlated quite well by using the present parameters. The values of ρ_s/ρ_p for these groups are 1.2, 1.4, and 1.5, respectively. For $1/\rho_p << 1$, the agreement with our "thin sheath" approximation is seen to be fairly close (typically, within a factor of 2; better than that, on the average). It should be noted that for six of the points shown in Fig. 4 the condition $1/\rho_p > 22/\omega^2$ was not satisfied, so that the viscous boundary layer was thicker than the sheath. These points are marked by a bar. Their location does not differ from the general trend.

At the higher values of $1/\rho_p$, the experimental data show values of $\mathcal{J}/\mathcal{J}_L$ that are larger than unity. It is conceivable that these data are influenced by ion production. The production parameter P is proportional to $1/\rho_p$ (see the preceding subsection), and may have assumed values of order one for experiments with large $1/\rho_p$. Any definitive conclusions about this possibility would have to be based on the experimental values of N_∞/a, which are not available from Ref. 13.

IV. Application to Cylindrical Probes

The method described in the previous section can also be applied to cylindrical probes. In the interest of brevity, only some of the main results are given here. Equation (29) remains unchanged while Eqs. (30) become

$$d\rho/dt = (1-\rho_p^2/\rho^2)\cos\theta + \omega R_i^{-2}\partial\varphi_0/\partial\rho$$

$$d\theta/dt = -\rho^{-1}(1+\rho_p^2)\sin\theta + \omega R_i^2\rho^{-2}\partial\varphi_0/\partial\theta \qquad (46)$$

Equation (31) remains unchanged, while Eq. (32) becomes

$$\mathcal{J} = 2\rho_p \int_0^\pi j_p(\theta)\, d\theta \qquad (47)$$

The cylindrical analogs of Eqs. (33) and (34) are

$$\mathcal{J}_L = \pi\rho_p^2(-1+\rho_s^2/\rho_p^2) \qquad (48)$$

$$\Omega = \tfrac{1}{4}(1-\rho_s^2/\rho_p^2) + \tfrac{1}{2}(\rho_s^2/\rho_p^2)\ln(\rho_s/\rho_p), \qquad (49)$$

respectively. The asymptotic result for $1/\rho_p << 1$ now is $\mathcal{J}/\mathcal{J}_L = ((2/\pi\rho_s)$. The thin sheath results replacing Eqs. (36, 37, and 39-41) are, respectively

$$\delta(\theta=\pi) \equiv \rho_s(\theta=\pi) - \rho_p \approx (3^{1/2}/2)\rho_p^{5/4}\Omega^{1/2} \qquad (50)$$

$$j(\theta=\pi) \approx 3^{1/2}\rho_p^{1/4}\Omega^{1/2} \approx (9/8)\rho_p^4\Omega^2[\delta(\theta=\pi)]^{-3} \qquad (51)$$

$$d\gamma/d\alpha = -4\gamma/(\gamma-\cos\alpha)/\sin\alpha \qquad (52)$$

$$\mathcal{J} = 5.27\,\Omega^{1/2}\rho_p^{5/4} \quad \text{(thin sheath)} \qquad (53)$$

$$\mathcal{J}/\mathcal{J}_L = 0.593\rho_p^{-3/4} \quad \text{(thin sheath)} \qquad (54)$$

Theoretical results for $\mathcal{J}/\mathcal{J}_L$ as a function of ρ_p^{-1} at various values of Ω for cylindrical probes have been plotted in Fig. 6. They are quite similar to the corresponding results for spherical probes shown in Fig. 4.

In order to evaluate the ion density from experimental data, a procedure entirely similar to that described at the end of the preceding subsection may be followed. The only difference is that Eq. (42) must be replaced by

$$\mathcal{J}\Omega^{-2}\rho_p^2 = Ier_p/(\epsilon_0 kT_i D_i\omega^2) \qquad (55)$$

and Eq. (45) by

$$\Omega = 9.17(\Omega\rho_p)^{-1}(\mathcal{J}\Omega^{-2}\rho_p^{-2})^{-4/3} \qquad (56)$$

Experimental data with cylindrical probes in incompressible continuum flow were reported by Clements and Smy.[16] The data shown in Fig. 4 of Ref 16 are included in the present Fig. 6. These data were obtained with $\omega \approx 190$, $h_i/r_p \approx 0.4$, $\Omega \approx 26$, $ReSc_i \approx 5 \rightarrow 65$, $R_i \approx 0.9 \rightarrow 12$. They are seen to lie somewhat above the result of the first iteration. In this sense, the agreement is as good as could be expected.

Experiments with cylindrical probes in shock tubes were reported by French et al,[13] and by McLaren and Hobson.[17] The assumptions on which the present theory is based were generally satisfied in these experiments, except that the flow was slightly supersonic and hence compressible. We have found it interesting to compare also these experimental results

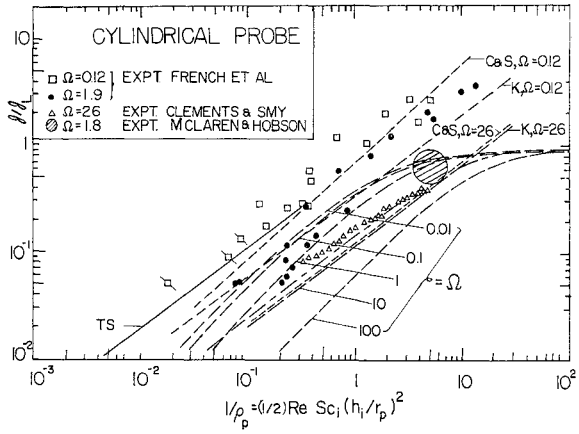

Fig. 6 $\mathcal{J}/\mathcal{J}_L$ as function of $1/\rho_p$ for cylindrical probe, at various values of the parameter Ω. TS (thin sheath) result based on Eq. (54), C&S results on Ref. 16, *K* results on Ref. 18, expt. French et al. on Ref. 13, expt. Clemands and Smy on Ref. 16, expt. McLaren and Hobson on Ref. 17.

with the present theory. The data plotted in Figs. 10 and 11 of Ref. 13 were converted to present variables by using the average values of ω and h_i/r_p indicated in the corresponding figure captions. This yielded $\Omega=0.12$ and $\Omega=1.9$ for the data with $\omega=12$, $h_i/r_p=0.1$ and $\omega=40$, $h_i/r_p=0.22$, respectively. The range of $ReSc_i$ was $3.2\rightarrow660$, while $R_i\approx0.2\rightarrow60$. The results are included in the present Fig. 6. For small values of $1/\rho_p$, the $\Omega=0.12$ data agree fairly well with the thin sheath result, while the $\Omega=1.9$ data agree fairly well with the result of the first iteration. In both cases, the agreement is typically within a factor of two, with the experimental data on the average being about 50% high. For $1/\rho_p\geq1$, the experimental results again yield values of $\mathcal{J}/\mathcal{J}_L$ that are larger than unity. Three points for which the viscous boundary layer was thicker than the sheath (i.e. for which $1/\rho_p<15/\omega^2$) are marked by a bar.

McLaren and Hobson[17] while not reporting any individual data points, state that their data are correlated by the formula $\mathcal{J}/\mathcal{J}_L=K(2/\pi\gamma)^{1/2}(M\rho_p)^{-1}(-1+\rho_s^2/\rho_p^2)^{-1}$, where K is a constant between 1 and 2, and γ the ratio of specific heats. Typical conditions were: shock Mach number $M_s=9.5$, initial pressure $p_1=133$ Pa (1 torr), freestream ion density $N_\infty=10^{10}\text{cm}^{-3}$, freestream temperature $T=8500$ K, freestream Mach number $M=1.31$, and probe potential $V_p=-5V$. The probe radius r_p was 0.0125 cm. Using these numbers, we find $\omega\approx7$, $h_i/r_p\approx0.5$, $ReSc_i\approx40$, $R_i\approx10$, $\mathcal{J}/\mathcal{J}_L=0.4$ to 0.8, $1/\rho_p\approx5$, $\Omega\approx1.8$. This result is seen to be in fair agreement with the other experimental data shown in Fig. 6. The theoretical results marked "C&S" and "K" are discussed in the next section.

V. Comparison with Other Theories

First of all, we briefly discuss the relation between the present theory and that of Lam.[2] Our basic Eqs. (1-3) agree with Lam's Eqs. (2.8-2.10), and our boundary conditions (4) are the same as those imposed by Lam.[2] Furthermore, our Eq. (7) for the ion density in the quasineutral region is equivalent to the equation given by Lam[2] for the outer region. Except for these points of agreement, the present analysis is basically different from that of Lam.[2] While we obtained $\phi_0=0$ in the quasineutral region, Lam[2] concluded that the potential in this region must be a nontrivial solution of Laplace's equation. In fact, Lam[2] criticized earlier work of Chung[18] and of Talbot,[19] who assumed the potential drop to occur entirely in the sheath. For highly negative probes, the present theory provides a justification of the latter assumption in terms of perturbation theory: the potential in the quasineutral region is identically zero to lowest order (ϕ_0), as well as to next highest order (ϕ_1). For incompressible flow we have $n_0=1$, in which case Eq. (8) shows that $\phi_2=0$, too. For $n_0\neq1$, we have $\phi_2\neq0$. Either way, the correct boundary condition along the edge of the sheath is $\varphi_0=0$. In analyzing the problem further, Lam[2] made the restrictive assumption that the sheath and the ambipolar diffusion region are confined to a thin layer adjacent to the body surface. This allows an important simplification: The coordinate normal to the body surface can be stretched, and most terms with derivatives along the body surface drop out of the equations. As a result, the problem can be solved for any value of the body potential.[2] This method of solution does not apply to the more general case of a "thick" sheath, i.e. a sheath not confined to a thin layer near the body surface. The latter case is of practical importance for small probes at a highly negative potential. The present paper shows that this case is amenable to treatment by perturbation theory, using the inverse of the dimensionless probe potential as the small parameter. Finally, the present work differs from that of Lam[2] in the ordering assumed for the thickness of the sheath and of the "ambipolar diffusion region." The latter region here is called the transition region, and is thin compared with the sheath thickness, whereas Lam's treatment concerns the opposite case.

Next, it is of interest to compare the present theoretical results with theoretical results obtained by Kulgein[20] and by Clements and Smy.[15,16] In deriving the latter results, the effect of convection within the sheath was left out of the account. This removes the mechanism by which ions can flow from the sheath back into the quasineutral region, so that all ions arriving at the sheath edge are collected by the probe. As explained in Sec. III, this model has merit when $1/\rho_p<<\Omega$ (electric effects dominate over convective effects). However, it is invalid when $1/\rho_p>>\Omega$, in which case it predicts values of $\mathcal{J}/\mathcal{J}_L$ larger than unity. The data of French et al.[13] agree with this prediction, but we believe that the agreement is fortuitous.

Kulgein's results[20] apply to cylindrical probes, and are based on the assumption that the sheath is circularly symmetric, with the current in the sheath being space-charge-limited. Only the forward half of the probe is assumed to collect current. The main equations (6) and (9) of Ref. 20 become in present notation

$$(\alpha-1/\alpha)\{(\alpha^2-1)^{1/2}-\alpha\ln[\alpha+(\alpha^2-1)^{1/2}]\}=\tfrac{1}{2}\pi\Omega^2\rho_p \quad (57)$$

$$\mathcal{J}/\mathcal{J}_L=(2/\pi\rho_s)(\alpha-1/\alpha)[(\rho_s/\rho_p)-(\rho_p/\rho_s)]^{-1} \quad (58)$$

where $\alpha\equiv r_s/r_0$. Equation (57) serves to determine α, while ρ_s/ρ_p in Eq. (58) follows from Eq. (49).

The approach of Clements and Smy[16] is basically identical to that of Ref. 20. However, these authors made two further simplifications, resulting in slightly different formulas. The simplifications are based on the assumption that $r_s/r_p>>1$, and consist of replacing the expression in curly brackets on the left hand side of Eq. (57) by $-\alpha\ln\alpha$, and of replacing $\alpha-(1/\alpha)$ by α. A corresponding theory for spherical probes is presented in Ref. 15. Some of the results it yields are included in Fig. 4. Clements and Smy[15,16] rightly drew attention to the large influence of even a small flow velocity U on the current collected, as compared to the no flow case.

VI. Discussion

The results of Sec. II show in a rigorous way that the equations governing the problem posed are those for an undisturbed quasineutral region, and an ion sheath region in which the ion flow is dependent on both convection and electric effects. To lowest order, the electric field and potential are zero at the edge of the sheath, while the ion current density follows from matching with the quasineutral region. There results a well-defined mathematical problem, the solution of which is difficult to obtain even for cylindrical or spherical probes. However, a closed form solution is

possible in the limit of small $1/\rho_p$ and small Ω (thin sheath solution). The latter result is in reasonably good agreement with the few experimental data available in this limit. For values of Ω that are not small, we have obtained a lower limit as well as an upper limit for the current collected. Available experimental data indeed fall between these limits for $1/\rho_p < 1$. It would be interesting to find numerical solutions of the partial differential equations describing the ion flow in the sheath under these conditions, in order to obtain precise results for the current collected. However, such solutions are considered outside the scope of the present paper. In any event, the present theory has shown that under the assumptions made, the many possible parameters of importance that were mentioned in Ref. 13 can be reduced to three, so that the results can be presented as a one-parameter family of curves.

One of the weaknesses remaining in the present results for spherical and cylindrical probes is the assumption that the neutral flow around the probe may be described by the potential flow equations. The resulting flow pattern is quite inaccurate near the rearward part of the probe. However, most of the current is collected on the forward part of the probe, and the errors in $\mathcal{J}/\mathcal{J}_L$ caused by this assumption are believed to be small. On the other hand, significant errors may be caused by assuming that ion production is negligible. As indicated in Sec. III, it is possible to take such production into account (see also Ref. 11). It appears worthwhile to further investigate the case with ion production.

The results of the approximate theories described in Sec. V are in reasonably good agreement with experimental data. For small $1/\rho_p$, the main assumption underlying these theories, viz., the neglect of convection inside the sheath, is justified. This assumption is no longer valid when $1/\rho_p$ is large. The few data available for large $1/\rho_p$ show values of $\mathcal{J}/\mathcal{J}_L$ that are anomalously high when compared with the predictions of rigorous incompressible theory. As a consequence, the approximate theories happen to correlate these data rather well.

Besides the need for further theoretical work indicated in the preceding lines, further progress in the use of continuum electric probes would be greatly aided by the availability of additional experimental data covering a wide range of parameters. In obtaining these data, additional ionization caused by the presence of the probe should be either eliminated, or well understood. In any event, it appears feasible to use cylindrical and spherical probes for convenient and quite accurate measurements of local ion density in flowing continuum plasmas.

Acknowledgment

This work was partly supported by a grant from the Ford Motor Company.

References

[1]Chung, P.M., Talbot, L., and Touryan, K.J., "Electric Probes in Stationary and Flowing Plasmas: Part II: Continuum Probes, *AIAA Journal,* Vol. 12, Feb. 1974, pp. 144-154.

[2]Lam, S.H., "A General Theory for the Flow of Weakly Ionized Gases," *AIAA Journal,* Vol. 2, Feb. 1964, pp. 256-262.

[3]Van Dyke, M., *Perturbation Methods in Fluid Mechanics,* Academic Press, New York, N.Y., 1964.

[4]Cole, J., *Perturbation Methods in Applied Mathematics,* Blaisdell Publishing Co., Waltham, Mass., 1968.

[5]Nayfeh, A.H., *Perturbation Methods,* Wiley, N.Y., 1973.

[6]deBoer, P.C.T., "Ion Boundary Layer on a Flat Plate," *AIAA Journal,* Vol. 11, July 1973, pp. 1012-1017.

[7]deBoer, P.C.T., and Ludford, G.S.S., "Spherical Electric Probe in a Continuum Gas," *Plasma Physics,* Vol. 17, Jan. 1975, pp. 29-43.

[8]Su, C.H. and Lam, S.H., "Continuum Theory of Spherical Electrostatic Probes," *The Physics of Fluids,* Vol. 6, Oct. 1963, pp. 1479-1491.

[9]Lamb, H., *Hydrodynamics,* Dover Publications Inc., N.Y., 1945.

[10]Smirnov, V.I., *A Course in Higher Mathematics,* translated by Brown, D.E., Vol. IV, Chap. III, Pergamon Press, New York, N.Y., Addison-Wesley Publishing Co., Inc., Reading, Mass., 1964.

[11]David, T.S., "Spherical and Cylindrical Electric Probes in a Continuum Flowing Plasma," Ph.D. Thesis, Cornell University, 1971.

[12]deBoer, P.C.T. and Johnson, R.A., "Theory of Flat-Plate Ion Density Probe," *The Physics of Fluids,* Vol. 11, April 1968, pp. 909-911.

[13]French, I.P., Hayami, R.A., Arnold, T.E., Steinberg, M., Appleton, J.P., and Sonin, A.A., "Calibration and Use of Electrostatic Probes for Hypersonic Wake Studies, *AIAA Journal,* Vol. 8, Dec. 1970, pp. 2207-2214.

[14]deBoer, P.C.T., Johnson, R.A., and Grimwood, P.R., "Electric Ion-Collecting Probes Governed by Convection and Production, *Proceedings of the VIIth International Shock Tube Symposium,* University of Toronto Press, Toronto, Canada, 1970, pp. 795-819.

[15]Clements, R.M. and Smy, P.R., "Anomalous Currents to a Spherical Electrostatic Probe in a Flame Plasma, *British Journal of Applied Physics* (*Journal of Physics, D.*), Series 2, Vol. 2, 1969, pp. 1731-1737.

[16]Clements, R.M. and Smy, P.R., "Electrostatic-Probe Studies in a Flame Plasma," *Journal of Applied Physics,* Vol. 40, Oct. 1969, pp. 4553-4558.

[17]McLaren, T.I. and Hobson, R.M., "Initial Ionization Rates and Collision Cross Sections in Shock-Heated Argon," *The Physics of Fluids,* Vol. 11, Oct. 1968, pp. 2162-2172.

[18]Chung, P.M., "Electrical Characteristics of Couette and Stagnation Boundary-Layer Flows of Weakly Ionized Gases," *The Physics of Fluids,* Vol. 7, Jan. 1964, pp. 110-120.

[19]Talbot, L., "Theory of the Stagnation-Point Langmuir Probe," *The Physics of Fluids,* Vol. 3, Mar. 1960, pp. 289-298.

[20]Kulgein, N.G., "Ion Collection from Low-Speed Ionized Gas," *AIAA Journal,* Vol. 6, Jan. 1968, pp. 151-152.